

The AVO modelling volume

Brian H Russell, Hampson-Russell Software, Calgary, Alberta, brian@hampson-russell.com

Laurence R. Lines, University of Calgary, Calgary, Alberta, lines@geo.ucalgary.ca

Keith W. Hirsche, Hampson-Russell Software, Calgary, Alberta, keith@hampson-russell.com

Janusz Peron, Hampson-Russell Software, Houston, Texas, jperon@hrs-us.com

Daniel P. Hampson, Hampson-Russell Software, Calgary, Alberta, dan@hampson-russell.com



Summary

An AVO modelling scheme is proposed in which we create a 3D volume of modelled CDP gathers by varying two physical parameters, one in the in-line direction, and one in the cross-line direction. This 3D volume is then processed using conventional AVO analysis techniques, and the results are interpreted using time or structure slices. Two examples are presented. The first involves P-wave velocity change in one direction versus S-wave velocity change in the other. In the second, we change porosity in one direction against water saturation in the other, using the Biot-Gassmann equations to perform the modelling. In the first example, an excellent fit is obtained between actual and expected results. In the second example, the fit is encouraging, but far from perfect. This study has therefore motivated future research into the use of multi-attribute statistical methods on this problem

Introduction

AVO analysis generally involves the computation of several independent attributes from prestack seismic data, such as near and far stack, intercept and gradient, on μ -rho and λ -rho. However, due to the non-uniqueness of seismic data, there are a large number of possible geological models that can be postulated that will all fit the results of such an analysis. For this reason, it is important to perform modelling to try and better understand the information contained in observed seismic data. This is traditionally done by creating a model from the observed well logs, perturbing a single parameter, and observing the results. In this paper, we propose a straightforward method for creating multiple AVO models, which we call the AVO modelling volume.

The AVO modelling volume is created by choosing two physical parameters of interest, and allowing each to change in a systematic fashion, one in the in-line direction of a 3D volume, and the other in the cross-line direction. These parameters could consist of two elastic constants, such as P-wave velocity, S-wave velocity, Poisson's ratio or density; or two parameters that affect these elastic constants, such as porosity, saturation, permeability, temperature or pressure. When the modelling is complete, we have produced a cube of multi-offset AVO synthetic gathers, each with a different combination of physical parameters. This cube can then be processed in a traditional fashion, and the results interpreted. We will look at two examples in this paper: P-wave velocity against S-wave velocity, and porosity against water saturation.

Model 1 - V_p vs V_s

As a first example of the AVO modelling volume, we will perturb a three layer model. The model consists of a first and third layer of equal elastic parameters ($\rho = 2.11$ g/cc, $V_p = 2250$ m/s, $V_s = 1125$ m/s, $\sigma = 1/3$) and a second layer which will be allowed to change. The two parameters to be changed will be P-wave velocity and S-wave velocity, and the density will be held constant in all layers. The layer thickness is set 50 meters to minimize the effect of thin bed tuning, and a 25 Hertz Ricker wavelet used in the modelling process. Also, the far offset used is 500m, equal to the depth to the top layer. A 6 x 6 cube of modeled gathers is then created by allowing P-wave velocity to vary from 2000 m/s to 2500 m/s in increments of 100 m/s, and S-wave velocity to vary from 1000 m/s to 1250 m/s in increments of 50 m/s. This creates 36 gathers with V_p/V_s ratios varying from 5/2 to 8/5, and Poisson's ratios, σ , varying from 0.18 to 0.40. In fact, the V_p/V_s and Poisson's ratios form diagonal lines of constant value from the top right of the grid to the bottom left. That is, $V_p=2500$ m/s and $V_s=1250$ m/s gives the same value as $V_p=2400$ m/s and $V_s=1200$ m/s, and so on.

The modelling algorithm used is a primaries-only scheme in which the amplitudes are computed using the Zoeppritz equations, ray-tracing is used to compute the event traveltimes, and the final model is created by applying an NMO correction. The advantage of this modelling scheme is that it is fast and efficient, but the disadvantages are that we ignore the effects of converted waves, anelasticity, and anisotropy. These are all options that could, and should, be used for other modelling examples, for comparison with the simplest case. Before showing the results, let us review the linearized theory of AVO.

The intercept and gradient can be written in linearized form as (Aki and Richards, 1980, Wiggins et al, 1983):

$$R(\theta) = A + B \sin^2 \theta + C \sin^2 \theta \tan^2 \theta, \quad (1)$$

where

$$A = R_{P0} = \frac{1}{2} \left[\frac{\Delta V_P}{V_P} + \frac{\Delta \rho}{\rho} \right],$$

$$B = \frac{1}{2} \frac{\Delta V_P}{V_P} - 4 \left(\frac{V_S}{V_P} \right)^2 \frac{\Delta V_S}{V_S} - 2 \left(\frac{V_S}{V_P} \right)^2 \frac{\Delta \rho}{\rho},$$

$$C = \frac{1}{2} \frac{\Delta V_P}{V_P}.$$

and

The third term, C, is small for angles less than 30 degrees, and is usually dropped, although this is not a good idea for long offset data. From the above equations, note that the intercept slice in Figure 3(a) is responding to changes in P-wave velocity (recall that we held density constant, so $\Delta \rho / \rho = 0$), and the gradient is responding to the V_P/V_S ratio. A common method of AVO analysis is to produce weighted sums or differences of the intercept and gradient. If we assume that $V_P/V_S = 2$, it can be shown that:

$$\frac{A - B}{2} = R_{S0} \quad (2)$$

and

$$\frac{A + B}{2} = R_{P0} - R_{S0} \quad (3)$$

where

$$R_{S0} = \frac{1}{2} \left[\frac{\Delta V_S}{V_S} + \frac{\Delta \rho}{\rho} \right], \quad R_{P0} = \frac{1}{2} \left[\frac{\Delta V_P}{V_P} + \frac{\Delta \rho}{\rho} \right]$$

Figure 1 shows the results of the modelling for all 36 models, with V_P changing in the vertical direction, and V_S changing in the horizontal direction. Although the expected trends are present in Figure 1, with V_P controlling the zero-offset reflection coefficient, and V_P/V_S controlling the change in amplitude as a function of offset, there is a lot of information to assimilate in this figure.

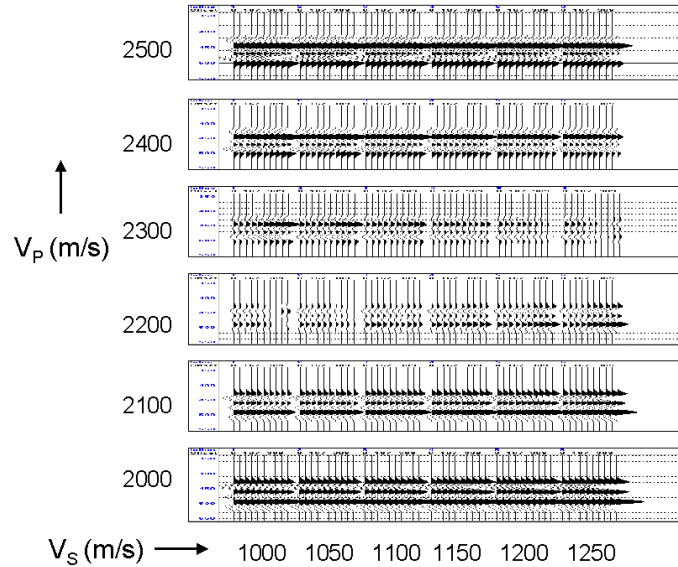


Figure 1. The result of the first AVO modelling volume, where the in-line (horizontal) direction represents change in S-wave velocity and the cross-line direction (vertical) represents changes in P-wave velocity.

The next step is therefore to process the modelling cube for two separate attributes and analyze these results. Although there are many possible pairs of attributes that could be chosen, we decided to use the intercept and gradient attributes, as they are the most common attributes used in current practice. The processed volumes were then sliced at a time of 444 msec, which corresponds to the maximum on the first event (trough or peak). The slices through the intercept and gradient volumes are shown in Figures 2(a) and 2(b), respectively. Notice that the intercept slice shows a horizontal striping, and the gradient slice shows roughly diagonal striping, as we would expect from the preceding review of AVO theory.

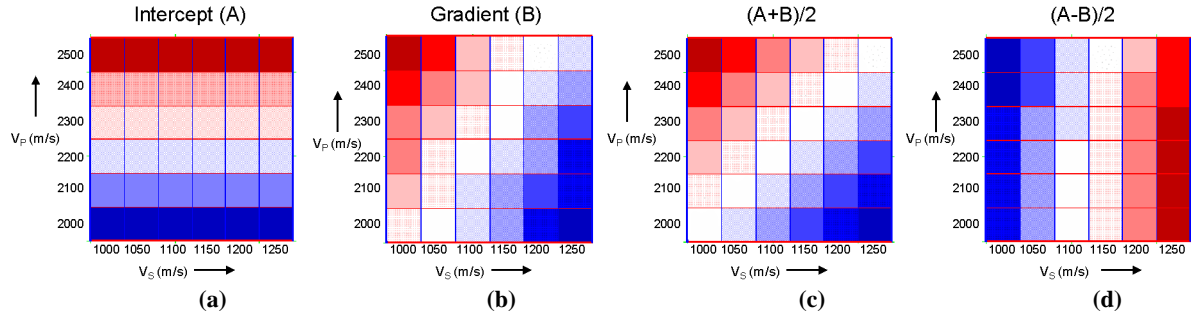


Figure 2. Time slices from the (a) intercept, (b) gradient, (c) scaled sum of intercept and gradient and (d) scaled difference of intercept and gradient computed from the gathers in Figure 1. Note that Red = positive and Blue = negative amplitudes.

We next create the sum and difference of the intercept and gradient slices shown in Figures 2(c) and 2(d). Notice that the summed slice shows perfect diagonals since it represents the difference between changes in P-wave velocity and S-wave velocity. The difference slice shows vertical striping rather than horizontal striping, since it is responding to changes in the S-wave velocity. The vertical striping is not perfect since the V_p/V_s ratio is not constant and equation (2) is only strictly valid when $V_p/V_s = 2$ and the third term in equation (1) is negligible. Note that the sum $A+B$ can also be thought of as the scaled change in Poisson's ratio, if we start with Shuey's linearized approximation, involving V_p , ρ and Poisson's ratio σ .

Now that we have looked at this simple problem, let us go on to the more complex problem of porosity versus water saturation, where all three physical parameters (V_p , V_s , and density) will change for each grid cell.

Model 2 - Porosity Versus Water Saturation

In our second example, we will model porosity versus saturation. Again, we create a three layer model, where only the middle layer is allowed to vary. The porosity and saturation were computed using the Biot-Gassmann equations. The water saturation was varied from 0 to 100% in increments of 10%, and the porosity was varied from 23% to 33%, in increments of 1%. This created a cube of 11 x 11 gathers for a total of 121 gathers. Figure 3 shows the prestack seismic response of the model, for two in-lines. Figure 3(a) shows in-line 1, which is for a constant water saturation of 0%, and variable porosity. Notice that the gradient on the trough at 450msec is negative along the whole line (that is, the trough gets more negative), and that the intercept gets larger as we move to higher porosity. Figure 3(b) is for in-line 11, which represents a water saturation of 100%. Notice that the polarity is reversed from in-line 1, but that the gradient is still negative (that is, the peak at 450msec is decreasing). In this case, the intercept decreases as we move to higher porosity.

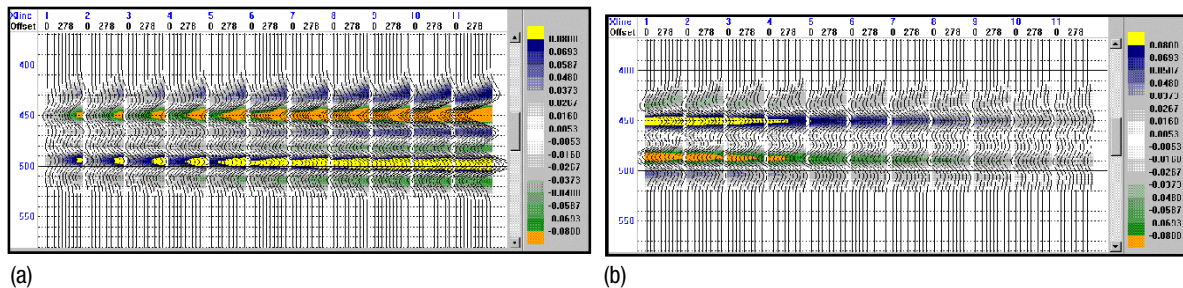


Figure 3. The modelled gathers from (a) in-line 1 at 0% water saturation, and (b) in-line 11 at 100% water saturation. In both cases, the gradient is negative on the top event, although the polarity, and therefore the intercept, is reversed between the two sets of gathers. In both cases the porosity goes from 23% on the left to 33% on the right.

Next, we will look at the AVO responses from this dataset. Figures 4(a) and 4(b) show time slices at a time of 450 ms (the trough from the first event on lines 1 through 10, and the peak on line 11) from both the intercept cube and the gradient cube. Notice that both the intercept and gradient show roughly horizontal "stripes" except at the 100% water saturation point, where a strong vertical "stripe" is evident. This indicates that porosity is the controlling factor for water saturation less than 100% (i.e. when gas is present) but that a water saturation of 100% will dominate the seismic response. That is, the porosity and water saturation effects are strongly coupled. Let us now see if there is any combination of intercept and gradient that will de-couple the porosity and water saturation effects.

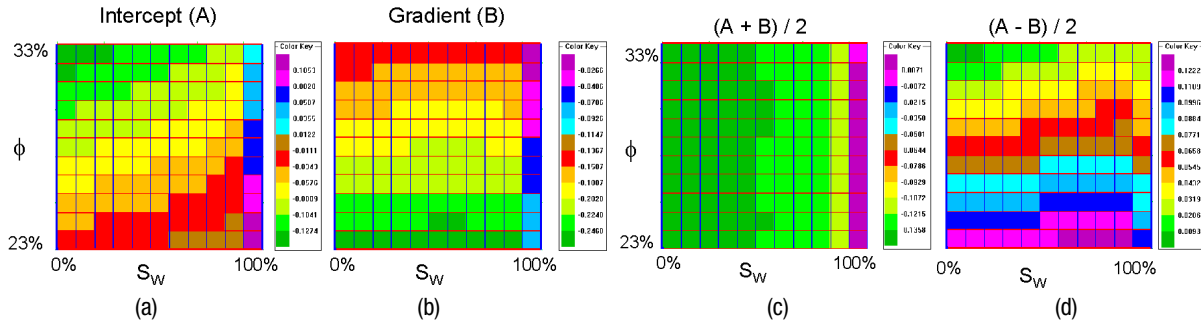


Figure 4. Time slices at 450 ms from the modelled volume of Figure 3, where (a) shows intercept alone, (b) shows gradient alone, (c) shows the scaled sum of intercept and gradient, and (d) shows the scaled difference of intercept and gradient.

Figures 4(c) and 4(d) shows time slices through the sum of intercept and gradient (which we have shown is roughly equivalent to the change in Poisson's ratio) and the difference between intercept and gradient (which we have shown is roughly equivalent to the zero-offset shear wave reflectivity). Notice that the sum of A and B is starting to display vertical "striping", indicating that it is responding to the change in water saturation, whereas the difference of A and B is displaying horizontal striping, indicating that it is responding to porosity. From a physical point of view, this makes sense, since water saturation is related to Poisson's ratio, and porosity change to reflectivity. However, the results are certainly not as conclusive as we would like.

As a further check on the relationship between the AVO attributes and the changes in porosity and water saturation, we would suggest using a statistical multi-attribute approach (Hampson et al, 2000). In this method, either a multi-linear regression or neural network technique can be used to predict combinations of attributes that best match a particular reservoir parameter. This approach is being currently worked on and will be the subject of a future paper.

Acknowledgements

This talk was originally given as a presentation at the 2000 CREWES consortium meeting in Calgary. We acknowledge the support of the CREWES sponsors and our colleagues at the University of Calgary.

Conclusions

In this paper we have discussed a new method for performing two parameter AVO modelling. This method involves creating a pseudo-3D volume of modeled gathers in which variations in one parameter are changed along the in-line direction, and variations of the other parameter are changed along the cross-line direction. Treating the resulting data as a 3D volume, and processing it with standard AVO analysis techniques, will reveal subtle effects that would otherwise be difficult to visualize. Our first model, which changed P-wave velocity versus S-wave velocity, gave us a better understanding of the various intercept/gradient methods. Our second example, which varied porosity against water saturation for a gas sand, gave us an understanding of the coupling between these two reservoir parameters. In our second example, the attribute combinations were not quite as effective as we would hope, although some indication of porosity and water saturation were revealed. Current research is underway to improve this prediction using statistical multi-attribute techniques.

References

Aki, K., and Richards, P.G., 1980, Quantitative seismology: Theory and methods: W.H. Freeman and Company.
 Hampson, D., Todorov, T., and Russell, B., 2000, Using multi-attribute transforms to predict log properties from seismic data: Exploration Geophysics, 31, 481-487.
 Shuey, R.T., 1985, A simplification of the Zoeppritz equations: Geophysics, 50, 609-614.
 Wiggins, R., Kenny, G.S., and McClure, C.D., 1983, A method for determining and displaying the shear-velocity reflectivities of a geologic formation: European Patent Application 0113944.